ACS OMEGA

Open Access

http://pubs.acs.org/journal/acsodf

Article

Removal of Toxic Lead from Wastewater by *Lupinus albus* Seed Hull

Amal A. Abdel Hafez, Hisham S. M. Abd-Rabboh, Ali M. Al-Marri, and Awaad H. A. Aboterika*

Cite This: *ACS Omega* 2023, 8, 42622−42631

Read Online

ACCESS | Metrics & More | Article Recommendations | Supporting Information

ABSTRACT: In this work, we address two concerns at once: waste reduction and the development of a lead removal adsorbent. The potential of *Lupinus albus* seed hull (LSH) powder as an efficient, innovative, and economical adsorbent for Pb(II) absorption was examined in this study. Fourier transform infrared spectroscopy, energy-dispersive X-ray spectroscopy, and scanning electron microscopy investigations were used to determine the structural and morphological properties of the LSH adsorbent. The adsorption process was studied in batch mode with multiple process variables (adsorbent dosage of 4.0−20 g/L; solution pH of 1.5−5.5; contact time of 15−70 min). By fitting the equilibrium data to the Langmuir isotherm model, the maximum adsorption capacity of Pb(II) was 357.14 mg/g at optimized pH (5.5), LSH dose (0.4 g), and interaction time (60 min) with starting Pb(II) concentration of 50 mg L^{-1}. As for the reaction kinetics, the pseudo-second-order model was shown to be a convenient match. LSH can be reused after four desorption/adsorption cycles and has a high potential for eliminating Pb(II) from wastewater.

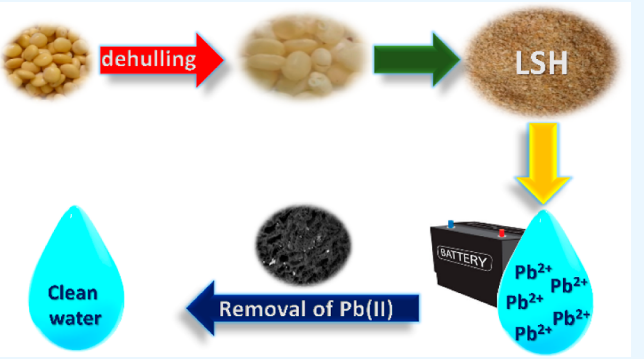

1. INTRODUCTION

All living creatures require water as a fundamental resource in order to continue their life. Access to clean and safe drinking water has recently grown to be a serious concern, especially in developed and developing countries because of industrial development, uncontrolled urbanization, and water contamination from industrial effluents and household waste. Lead, nickel, copper, zinc, and other heavy metals are frequently found in industrial effluents.[1,2]

Water containing lead (Pb) ions is extremely harmful to both humans and the environment. The production of batteries, pigments, and ammunition is one of the businesses that use lead, as do the welding, steel, and electroplating operations.[3,4] Lead accumulation in the human body can gravely damage the brain system, tissues, and organs.[5,6] The World Health Organization establishes a maximum of 0.01 mg/L for Pb(II) in drinking water.[7]

To eliminate heavy metal ions from contaminated water, many techniques have been developed including adsorption, ion exchange, membrane filtration, electrochemical approaches, flotation, and chemical precipitation. Numerous techniques have disadvantages, including high initial and ongoing expenses, the need for additional chemicals and energy, poor performance for diluted wastewater, and the production of dangerous byproducts.[8] Adsorption is one of the techniques that is particularly appealing due to its simple operation and great efficacy in treating water contaminated with low quantities of heavy metals.

As the world's population grows, so does the amount of agricultural waste produced. These wastes are largely unutilized, mismanaged, or underutilized for a variety of valuable applications. Flowers, fruit shells, fruit peels, vegetable peels, and other agricultural wastes with little commercial value are generated on a daily basis.[9] Due to their abundance in nature, renewal, zero toxicity, ease of conversion, and preparation with simple methods, waste peels from agricultural areas are suitable bioadsorbents for the elimination of Pb(II).

A number of the bioadsorbents, e.g., cotton hull,[10] banana peel,[11] cucumber peels,[5] mangosteen peel,[12] almond shells, hazelnut shells,[13] mango peel,[14] rice hull,[15] peanut hulls,[16] rapeseeds,[17] and potato peel[18] are the waste peels used to remove Pb(II).

The Fabaceae plant genus *Lupinus* includes the *Lupinus albus* species, which is primarily mature in Africa, northern Europe, Australia, and the Mediterranean region. Over the previous three decades, Australia has been the world's greatest lupine grower, accounting for over 70% of global output.[19,20] To make edible seeds from the *Lupinus albus* seeds, the seeds must be initially roasted before being soaked for 3−5 days in flowing water. Most members of the lower socioeconomic

Received: July 23, 2023
Revised: October 18, 2023
Accepted: October 24, 2023
Published: November 6, 2023

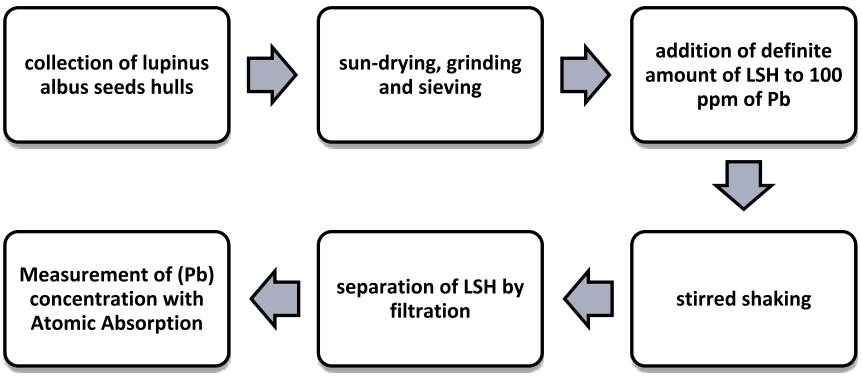

Figure 1. Schematic representation of the experimental process.

strata ingested the edible seeds, and they were also used as a traditional remedy by removing the shell and peel. It is utterly uneconomical to dispose of the hulls as waste in this manner.[20]

The coat (hull) of *Lupinus albus* seeds makes up about 25% of the total weight of the seed and is predominantly made up of phytochemicals like polyphenols and nonstarch polysaccharides.[21]

As far as we know, no research has addressed the use of the waste hulls of *Lupinus albus* as an adsorbent to eliminate heavy metals. In this study, *Lupinus albus* seed hull (LSH) was evaluated as a novel bioadsorbent for the elimination of Pb(II) from aqueous media. Therefore, we attempted to characterize LSH and study its potential as an adsorbent. The outcomes of several analytical method characterizations, adsorption kinetics, isotherms, and reusability of LSH for the removal of Pb(II) ions from wastewater are discussed.

2. EXPERIMENTAL SECTION

2.1. Materials. Sigma-Aldrich provided all of the analytical-grade compounds that were used. For adjusting the solution's pH to the required value, sodium hydroxide and nitric acid solutions were utilized. A synthetic stock solution of $Pb(NO_3)_2$ was prepared in ion-free water [Millipore Super Q system (resistivity of 18.2 MΩ)].

2.2. LSH Preparation. After the *Lupinus albus* seeds were burst with a plate grinder and the hulls were mechanically removed from the cotyledon portion, the hulls of the *Lupinus albus* seeds were collected. The *Lupinus albus* seed hulls underwent a deionized water wash, 105 °C drying for 24 h, and blending (Figure 1). The LSH was crushed using a Retsch laboratory mill type PM 100 (manufactured by Retsch GmbH, Haan, Germany) and sieved with 0.5 mm holes. All solutions resulting from all experiments were passed through a membrane filter (0.45 μm), and the filtrate was examined.

2.3. Instrumentation. The determination of lead was carried out by FAAS using a GBC Scientific Equipment model (Savant AA), with a lead hollow cathode lamp. Table S1 summarizes the experimental parameters of the spectrometer for the lead determination.

Fourier transform infrared (FT-IR, Bruker ALPHA II, Germany) was used to acquire the infrared spectra. The surface micromorphology of materials was investigated using a Quanta FEG-250 FEI scanning electron microscope. The elemental composition was checked by using an Apollo X SDD energy-dispersive spectrometer. Brunauer−Emmett−Teller isotherm (BET) is employed by Quantachrome's NOVAtouch LX2 pore and surface area analyzer to calculate the precise surface area.

2.4. Measurement of pH_{zpc}. A 100 mL portion of 0.01 N NaCl solutions was prepared and added to a succession of Erlenmeyer flasks, with their pH ranging between 2.0 and 12.0 using 0.01 N HCl and 0.01 N NaOH solutions, as needed. The first solution's pHs were determined using a pH meter and labeled $pH_{initial}$. To each flask was added 0.1 g of the LSH after achieving a constant initial pH value. After 24 h, the pH of the solution was recorded as pH_{final}. By plotting the difference in pH ($pH_{final} - pH_{initial}$) against $pH_{initial}$, the pHzpc of the LSH was determined at the point of equality between the $pH_{initial}$ and pH_{final}.

2.5. Batch Adsorption Study. *2.5.1. Interaction Time Impact.* Conical flasks having 0.4 g of LSH received aliquots (25.0 mL) of a solution with 50 mg L^{-1} of Pb(II). The mixtures were stirred for 15, 40, 50, 60, and 70 min at a speed of 150 rpm and 25 °C. Filtration was used to separate the LSH, and then atomic absorption was used to estimate the amount of Pb(II) present in the filtrate.

2.5.2. LSH Dosage Impact. Various 250 mL flasks received LSH transfers in the range of 0.1−0.5 g. Pb(II) solution in aliquots of 25.0 mL (50.0 mg L^{-1}) was added. After being sealed, the flasks were set in a shaking bed for a continuous equilibration period of 1 h. Atomic absorption spectrometry (AAS) was used to analyze the filtrate after filtration using a 0.45 μm filtration membrane.

2.5.3. Impact of the Solution pH. 25.0 mL of 50 mg L^{-1} of Pb(II) was transferred to the flasks. The beginning pHs were adjusted from 1.5 to 5.4 using solutions of 0.01 N HCl and 0.01 N NaOH, then 0.4 g pieces of LSH were added, and the mixture was allowed to reach equilibrium for 60 min at 25 °C.

2.5.4. Adsorption and Kinetic Isotherm Study. While keeping the LSH dosage constant, adsorption isotherms were produced with various initial Pb(II) concentrations. 25.0 mL aliquot of Pb(II) solution with starting concentrations at 10, 20.0, 30.0, 40.0, 50.0, and 60.0 mg L^{-1} were separately mingled with 0.4 g LSH in conical flasks at 25 °C. The mixes were given time to equilibrate before being filtered through a 0.45 μm membrane to determine the concentration of Pb(II) using AAS. In all tests, the change between the starting Pb(II) concentrations (C_o) and the equilibrium concentrations (C_e) was calculated to estimate the Pb(II) removal (%) by LSH and the adsorptive capacity (q_e) as follows in eqs 1 and 2, respectively

https://doi.org/10.1021/acsomega.3c05337
ACS Omega 2023, 8, 42622−42631

$$\text{removal efficiency}(\%) = \frac{(C_o - C_e)}{C_o} \times 100 \quad (1)$$

$$q_e = \frac{V}{m}(C_o - C_e)\ \text{mg/g} \quad (2)$$

where V denotes the overall volume of the tested solution (L), m is the amount of LSH (g), C_o is the starting concentration of the Pb(II) solution (mg L^{-1}), and C_e is the remaining Pb(II) concentration (mg L^{-1}).

The Langmuir model[22] has been effectively used in a variety of systems that have limiting or maximum sorption capacities. It is one of the earliest theoretical treatments of nonlinear sorption. The model presupposes homogeneous energies for adsorption onto the surface and a lack of adsorbate transmigration in the surface plane.

In eq 3, the Langmuir isotherm is presented

$$q_e = \frac{Q^o b C_e}{1 + b C_e} \quad (3)$$

where Q^o and b are adsorption capacity and energy of adsorption Langmuir constants, respectively.[23] Normally, eq 3 is inverted to linearize it, giving the result in the form shown here

$$\frac{1}{q_e} = \frac{1}{Q^o} + \frac{1}{bQ^o}\frac{1}{C_e} \quad (4)$$

By graphing $1/q_e$ vs $1/C_e$, eq 4 can also be used to analyze batch equilibrium data. If the data follow the Langmuir isotherm, then the result is a linear plot. Equation 5 defines dimensionless constant separation factor (R_L) as the main property of the Langmuir isotherm[24]

$$R_L = \frac{1}{1 + b C_o} \quad (5)$$

in which C_o is the starting concentration of Pb(II) and b is the adsorption Langmuir constant (L mg^{-1}). The R_L describes when the adsorption is linear ($R_L = 1$), unfavorable ($R_L > 1$), favorable ($0 < R_L < 1$), or irreversible ($R_L = 0$).[24]

Freundlich isotherm is the most commonly utilized nonlinear sorption model, and it has the following form[24]

$$q_e = K_F C_e^{1/n} \quad (6)$$

where n is the sorption intensity and K_F is the sorption capacity. Data from batch equilibrium studies are typically fitted using the logarithmic form of eq 6, which is presented below

$$\log\ q_e = \log\ K_F + \frac{1}{n}\log\ C_e \quad (7)$$

Pseudo-first-order[25] (eq 9), pseudo-second-order[26] (eq 11), and intraparticle diffusion model[27,28](eq 12), were used, respectively, to study adsorption kinetics.

The pseudo-first-order model can be illustrated as follows

$$\frac{dq_t}{dt} = k_1(q_e - q_t) \quad (8)$$

where k_1 is the pseudo-first-order constant (min^{-1}) and q_t is the amount adsorbed at time t. Equation 8 was transformed into a linear form by integrating at the borders as follows

$$\log(q_e - q_t) = \log q_e - \frac{k_1 t}{2.303} \quad (9)$$

The intercept was used to calculate the value of q_e, and the $\log(q_e - q_t)$ was used to calculate the rate constant, k_1.

The second-order kinetic model, which describes the chemical sorption, is given by eq 10

$$\frac{dqt}{dt} = k_2(q_e - q_t)^2 \quad (10)$$

where k_2 stands for the second-order kinetic constant (g/mg min). The boundary integration of eq 10 results in

$$\frac{t}{q_t} = \frac{1}{k_2 q_e^2} + \frac{t}{q_e} \quad (11)$$

Equation 12 could be used to study the Weber model[27] to explain how intraparticle diffusion affects the reaction

$$q_t = k_{id} t^{0.5} + C \quad (12)$$

where k_{id} is a Weber model factor and C is a factor associated with the depth of the boundary layer.

The most popular method for determining the best-fit model or the isotherm parameters is linear regression. In this procedure, the regression correlation coefficient, which is close to unity, is used to match the experimental data. However, it was discovered that linear regression may not be the best method for determining the ideal isotherm due to the inherent bias introduced by the linearization of the isotherm models. Nonlinear regression was used in this study to evaluate each model parameter. Five error functions were used to evaluate how well the equation fits the experimental data in order to enhance the technique.

1. Chi-square test, χ^2

$$\chi^2 = \sum_{i=1}^{n} \frac{(q_{e(\exp)} - q_{e(cal)})^2}{q_{e(\exp)}} \quad (13)$$

2. Average relative error, ARE

$$\text{ARE} = \frac{100}{n}\sum_{i=1}^{n}\left|\frac{q_{e(\exp)} - q_{e(cal)}}{q_{e(\exp)}}\right| \quad (14)$$

3. Sum of the square errors, ERRSQ

$$\text{ERRSQ} = \sum_{i=1}^{n}(q_{e(\exp)} - q_{e(cal)})^2 \quad (15)$$

4. Residual root-mean-square error, RMSE

$$\text{RMSE} = \sqrt{\frac{1}{n-2}\sum_{i=1}^{n}(q_{e(\exp)} - q_{e(cal)})^2} \quad (16)$$

5. Standard deviation of relative errors, S_{RE}

$$S_{RE} = \sqrt{\frac{\sum_{i=1}^{n}[(q_{e(\exp)} - q_{e(cal)}) - \text{ARE}]^2}{n-1}} \quad (17)$$

where n is the total number of observations in the experiment, $q_{e(cal)}$ is the equilibrium capacity calculated from the model (in mg/g), and $q_{e(exp)}$ is the equilibrium capacity derived from the experiment (in mg/g). The efficiency of the curve fitting increases with decreasing error function value.

https://doi.org/10.1021/acsomega.3c05337
ACS Omega 2023, 8, 42622−42631

2.6. Desorption Experiments. Desorption studies were performed for LSH recovery and reuse in the biosorption processes. In this study, the samples were stored for 60 min adsorption process, 0.4 g of LSH with 25.0 mL of Pb(II) (50 mg L^{-1}) at pH 5.5. Following that, LSH that had been loaded with Pb(II) was washed with a (0.1 M HCl) solution. After the adsorption process was completed, the material was washed and dried in an oven, and the Pb(II) content in the filtrate was measured by AAS. The adsorption efficiency was calculated by repeatedly performing the adsorption−desorption cycle until it reached a minimal and uneconomical value.

3. RESULTS AND DISCUSSION

3.1. Characterization of the LSH Adsorbent. BET N_2 adsorption−desorption isotherm was employed to estimate the average surface area and average pore size of LSH. The BET surface area of the LSH adsorbent was 119.531 m^2/g with an average pore size of 2.33 nm (Figure S1). The pHzpc is the state in which the amount of electric charge on the LSH's surface is zero. Figure 2 shows the pHzpc plot of the adsorbent

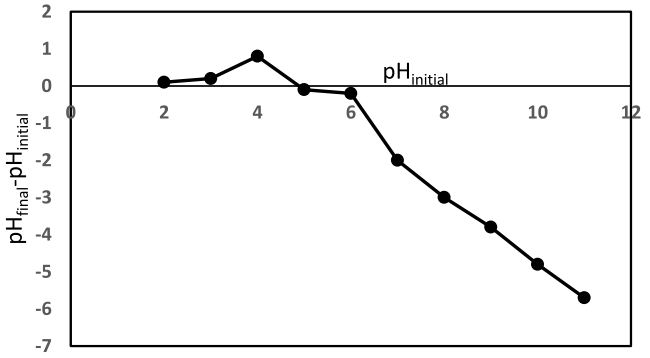

Figure 2. Plot for determination of the LSH point of zero charge.

(LSH). The pHzpc for LSH biosorbent was discovered to be 5.1. When pH > pHzpc, the LSH surface will become negatively charged, whereas it will become positively charged when pH < pHzpc.[29,30]

To identify the functional groups that are present on the surface of LSH, an FTIR spectral analysis was performed. The FTIR spectra of LSH and LSH-loaded Pb(II) are shown in Figure 3a,b. Four distinct peaks at 3287, 2921, 1600, and 1017 cm^{-1} were visible in the LSH's FTIR spectra (Figure 3a). The functional groups hydroxyl (−O−H) or amine (−N−H) are

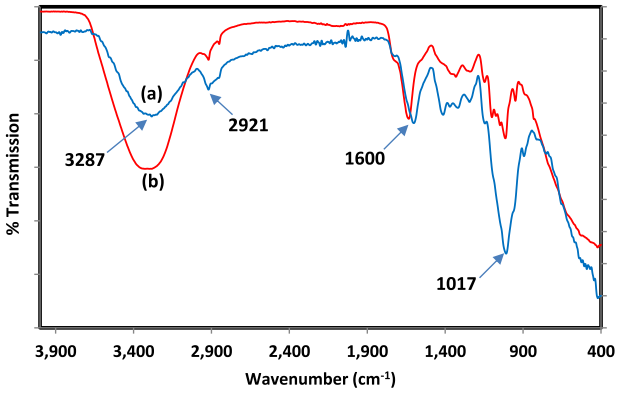

Figure 3. FTIR spectra for (a) raw LSH and (b) Pb(II)-loaded LSH.

represented by the wide and strong absorption peak located at 3287 cm^{-1}. The hydroxyl groups came from the LSH's remaining moisture, whereas the amine groups came from the LSH polypeptides.[31,32] The absorption peak at 2921 cm^{-1} reflects the presence of an alkane −C−H group. The peak at 1600 cm^{-1} is consistent with C═O stretching vibrations (carbonyl/carboxyl).[33] The C−N stretching (of amine groups) and the C−O stretching (of carboxylic acid and alcohol) are both represented by the peak at 1017 cm^{-1}.

Further comparison of the raw and Pb(II)-loaded LSH spectra lines was done in the study. Except for a slight shift in the peak positions of the four significant peaks at 3287, 2921, 1600, and 1017 cm^{-1} into 3310, 2918, 1630, and 1007 cm^{-1}, respectively, it was discovered that the spectra of the Pb(II)-loaded LSH displayed identical distinctive absorption peaks (Figure 3b). This might be due to the participation of hydroxyl, carbonyl, and carboxyl groups in the adsorption process.

Structure, exterior morphology (texture), chemical composition, and crystalline structure can all be learned by SEM.[34,35] Pre- and postadsorption SEM images of Pb(II) on LSH were taken at different magnifications to measure surface texture and adsorption porosity. Figure 4a,b shows the SEM images of raw LSH, and Figure 4c,d shows the SEM images of LSH after Pb(II) loading.

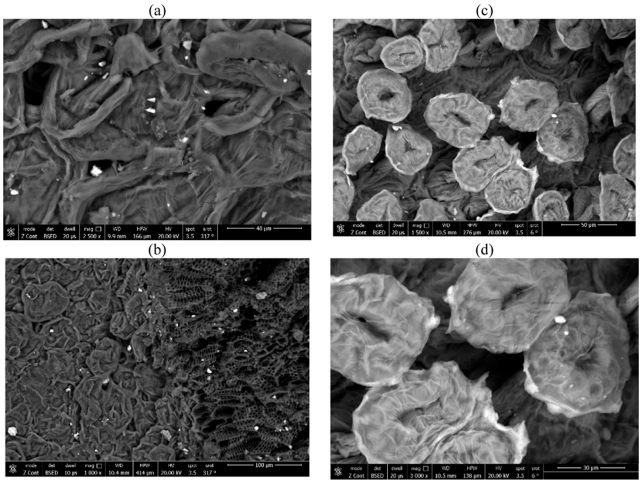

Figure 4. SEM for the native LSH (a,b) and Pb(II)-loaded LSH (c,d).

Figure 4a−d clearly shows the alteration in LSH morphology. Native LSH has macrosclereids (tubular) and cylindrical structures (Figure 4a,b), whereas LSH with Pb(II) enrichment has moderate irregularity in the structure. The surface of the LSH has likewise changed to a bright, white structure after Pb(II) adsorption (Figure 4c,d) which indicates that Pb(II) ions are present.

Using energy-dispersive peaks produced for the appropriate heavy metal ions, energy-dispersive X-ray (EDX) analysis verifies the presence of metal ions in the adsorbent. The EDX spectrum of native LSH and the Pb(II)-loaded LSH is shown in Figure 5a,b. The peak associated with the C and the O atoms can be seen in the LSH EDX analysis prior to adsorption (Figure 5a). With Pb(II) adsorption, adsorbed Pb(II) shows up as a peak in the EDX spectrum (Figure 5b). Consequently, the EDX analysis supports the Pb(II) adsorption onto the LSH adsorbent surface.

https://doi.org/10.1021/acsomega.3c05337
ACS Omega 2023, 8, 42622−42631

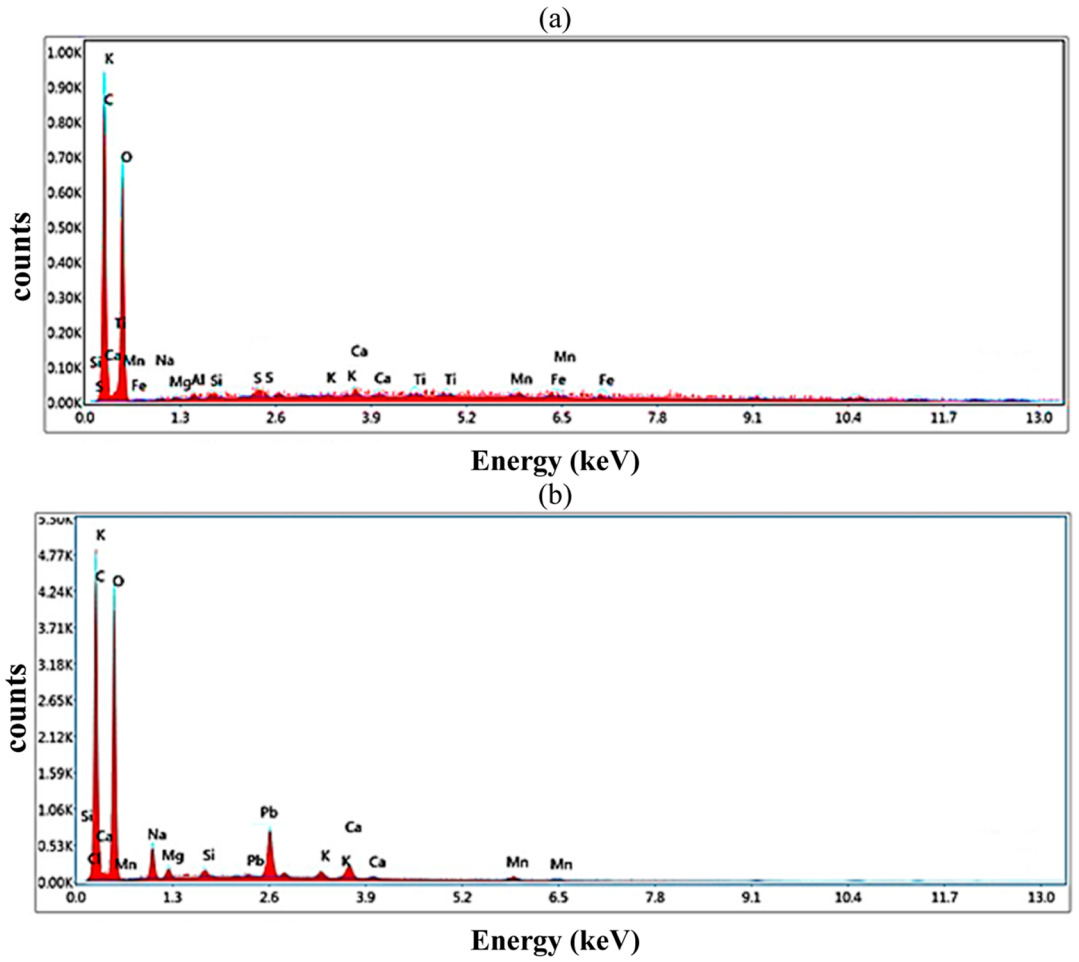

Figure 5. EDX for native LSH (a) and Pb(II)-loaded LSH (b).

3.2. Batch Adsorption Study. *3.2.1. Interaction Time Impact.* An important parameter to optimize for understanding the equilibrium condition is the contact time necessary for the maximal elimination of Pb(II). The results are displayed in Figure 6, and it is clear from the graph that the rate of Pb(II) adsorption by LSH was quick owing to the availability of vacant sites, with more than 90% of the Pb(II) ions being adsorbed in about 50 min. After that, the adsorption process reduced progressively and then stabilized at equilibrium. LSH had an equilibrium after 60 min, the equilibrium condition was reached because of repulsive interactions between the bulk phases and the metal ions adsorbed on the sorbent surface.[36] According to the findings, 60 min was enough time for LSH to reach equilibrium and remove 95.8% of Pb(II). Such type of adsorption has also been reported in the case of activated carbon.[37]

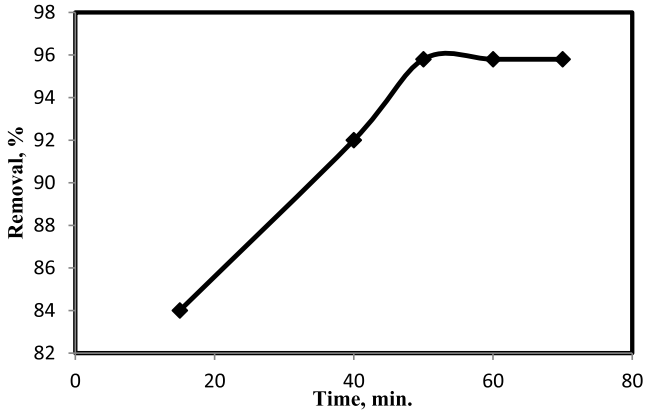

Figure 6. Impact of the interaction time on the removal of Pb(II) by LSH. Conditions: C_o, 50 mg/L; LSH dose, 0.4 g; pH, 5.5; and temperature, 25 °C.

3.2.2. LSH Dosage Impact. By conducting studies at pH 5.5 with a 50 ppm Pb(II) solution and adjusting the LSH dose in the range of 100−500 mg, it was possible to assess the effect of LSH dosage on the Pb(II) sorption. For LSH at doses of 100, 200, 400, and 500 mg/25 mL in the current investigation, Pb(II) removal was calculated to be 90, 93, 95, and 95.8% (Figure 7). The notably greater availability and simple accessibility of active sites for Pb(II) sorption on the LSH might be attributed to the increased Pb(II) adsorption at higher dosages. The maximum Pb(II) removal by LSH was seen at a dosage of 40 mg, and subsequent increases had no effect on sorption. So, the optimal value of the adsorbent dose for Pb(II) by LSH is 0.4 g.

3.2.3. Impact of the Solution pH. At pH values ranging from 1.5 to 5.5, the effect of pH on the Pb(II) removal rates by LSH was investigated. Pb(II) removal efficiency improved as pH values increased (Figure 8). Due to the repulsion between Pb(II) and the positively charged LSH surface, the removal yield of Pb(II) was determined to be 40% at pH 1.5. The removal rate of Pb(II) increased to 95.8% at pH 5.5 due to

https://doi.org/10.1021/acsomega.3c05337
ACS Omega 2023, 8, 42622−42631

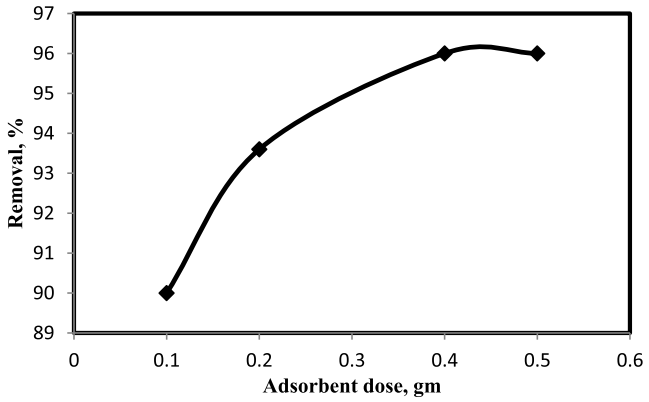

Figure 7. Impact of LSH dosage on the removal of Pb(II) by LSH. Conditions: C_o, 50 mg/L; time of interaction, 60 min; pH, 5.5; and temperature, 25 °C.

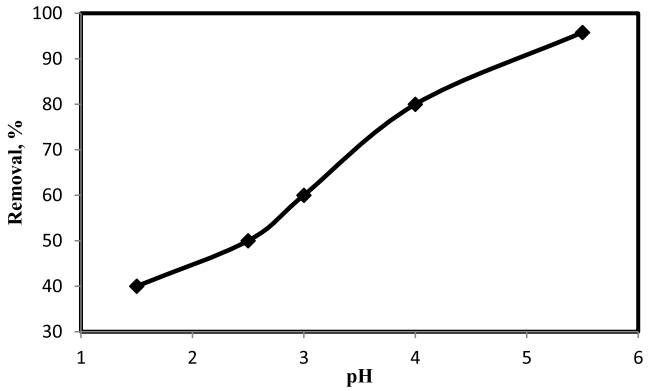

Figure 8. Impact of pH on the removal of Pb(II) by LSH. Conditions: C_o, 50 mg/L; LSH dose, 0.4 g; contact time, 60 min; and temperature, 25 °C.

attraction between Pb(II) and the negatively charged surface of LSH, which had a pHzpc of 5.1.[38] The optimal pH in the adsorption of Pb(II) by LSH is 5.5.

3.2.4. Adsorption Isotherm. The mass of adsorbent needed to remediate a contaminated stream is determined through equilibrium studies, which are crucial to the economics of sorption.[39] In accordance with the Langmuir model, a saturated monolayer of adsorbate molecules on the adsorbent surface corresponds to maximal adsorption. Specific adsorption $(1/q_e)$ against equilibrium concentration $(1/C_e)$ is plotted linearly (Figure 9) and has a correlation coefficient of 0.9997 (Table 1). 357.14 mg/g has been found to be the calculated Langmuir monolayer adsorption capacity. The fact that the dimensionless separation factor (R_L = 0.710) is in the range of 0 and 1 shows that Pb(II) adsorption onto LSH is an agreeable process.

Heterogeneous systems are frequently described by using the Freundlich model. The plot's Freundlich parameter, n = 0.9893, which is between 0 and 1 (Figure 10 and Table 1), indicates that the adsorption is favorable on the entire initial concentration range of Pb(II) ions.

Based on the R^2 values obtained from the various isotherms examined in this work, the Langmuir > Freundlich isotherms were the best-fit adsorption isotherms, and their corresponding R^2 values are 0.9997 and 0.9984, in the order of prediction precision.

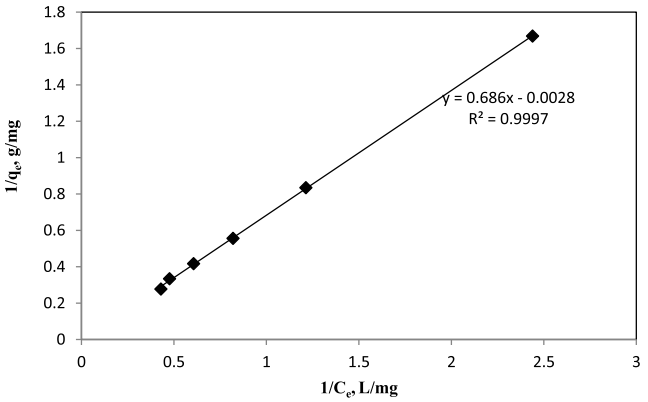

Figure 9. Langmuir isotherm plot of Pb(II) adsorption on LSH.

Table 1. Isotherm Variables for the Adsorption of Pb(II) on LSH

Langmuir	Q^o (mg/g)	357.14
	b (L/g)	0.0041
	R_L	0.710
	R^2	0.9997
	χ^2	0.011489
	ARE	1.62593
	ERRSQ	0.038171
	RMSE	0.154268
	S_{RE}	1.75036
Freundlich	K_F	1.46550
	N	0.98930
	R^2	0.99840
	χ^2	0.01531
	ARE	1.85706
	ERRSQ	0.054071
	RMSE	0.15979
	S_{RE}	2.03258

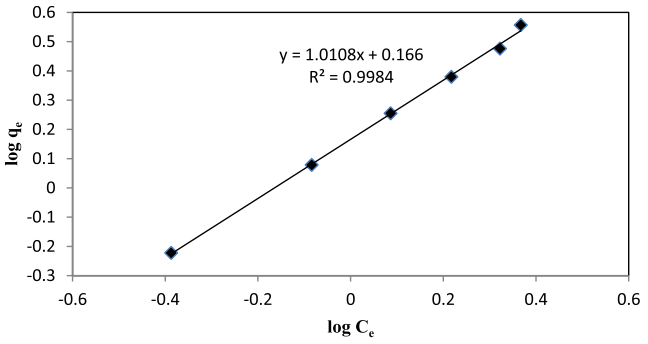

Figure 10. Freundlich isotherm plot of Pb(II) adsorption on LSH.

Table 1 includes the coefficient values for the Freundlich and Langmuir isotherms as well as the values of the various nonlinear method errors. In contrast to the Freundlich isotherm, the Langmuir isotherm has a greater correlation factor and lower error function values, which show that it more accurately represents the equilibrium data.

3.2.5. Adsorption Kinetics. It is essential to analyze sorption kinetics to understand the sorption behavior of LSH for Pb(II). Plots "$\log(q_e - q_t)$" − "t" and "t/q_t" − "t" in Figures 11 and 12 have been used to find the best fitted model for our experimental data.

https://doi.org/10.1021/acsomega.3c05337
ACS Omega 2023, 8, 42622−42631

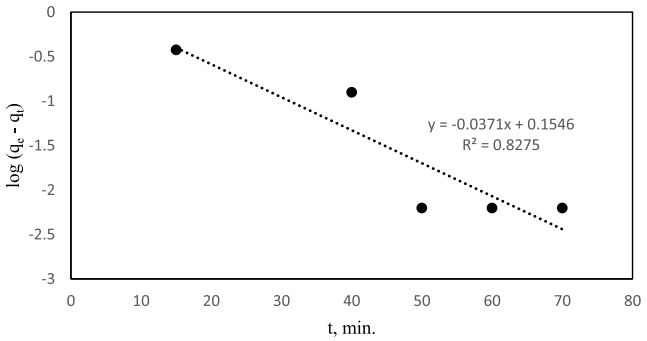

Figure 11. Adsorption kinetics of Pb(II) onto LSH by the pseudo-first-order reaction.

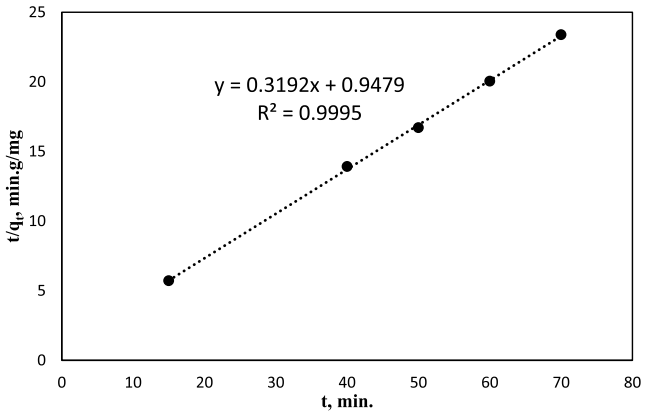

Figure 12. Adsorption kinetics of Pb(II) onto LSH by the pseudo-second-order reaction.

Table 2 shows that the "R^2" for the pseudo-second-order reaction (R^2 = 0.9812) is higher than the pseudo-first-order reaction. In addition, the calculated "q_e(cal)" value is reasonably close to the observed experimental "q_e(exp)" value, which implies that the adsorption behavior of Pb(II) on LSH obeys pseudo-second-order kinetics.

Table 2. Kinetic Variables for the Adsorption of Pb(II) onto LSH

pseudo-first-order kinetics	$q_{e(exp)}$ (mg/g)	3.000
	$q_{e(cal)}$ (mg/g)	1.427
	rate constant, k_1 (h^{-1})	0.0854
	R^2	0.8275
	χ^2	4.2392
	ARE	54.1610
	ERRSQ	12.2417
	RMSE	4.51577
	S_{RE}	58.8051
pseudo-second-order kinetics	$q_{e(cal)}$ (mg/g)	3.130
	rate constant, k_2 (g/mg h)	0.1076
	R^2	0.9995
	χ^2	0.00116
	ARE	0.64057
	ERRSQ	0.003392
	RMSE	0.063707
	S_{RE}	0.720146
intraparticle diffusion	C	2.36480
	rate constant, k_{id} (mg/g $h^{0.5}$)	0.08860
	χ^2	0.008748
	ARE	2.12440
	ERRSQ	0.02513
	RMSE	0.175704
	S_{RE}	2.442355

The effect of intraparticle diffusion on Pb(II) sorption was predicted by plotting q_t vs $t^{0.5}$. Figure 13 indicates that the plot

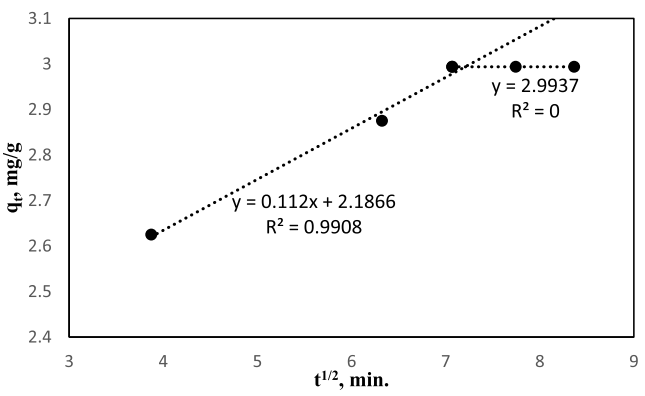

Figure 13. Intraparticle diffusion model for the sorption of Pb(II) onto LSH.

includes two linear lines showing two stages involved in Pb(II) sorption. The linearity in the first region indicated that Pb(II) diffused into the LSH surface across the bulk solution, whereas the linearity in the second region due to final equilibrium indicated that the intraparticle diffusion slowed down.

k_{id}, C, and R^2 values are set out in Table 2. The influence of Pb(II) transfer from solution to solid surface of LSH at the reaction was further investigated using an intraparticle diffusion model and a pseudo-second-order model. The pseudo-second-order model implies that chemical electrostatic interactions exist between the LSH surface and Pb(II) ions.[40]

Table 2 presents the results of calculating all of the parameters of various kinetic models and various nonlinear model errors. It has been demonstrated that the rate of adsorption follows a pseudo-second-order rate equation by comparing the values for the error and correlation coefficients.

3.2.6. Proposed Adsorption Mechanism. According to FTIR spectrum data shown in Figure 3, the biosorption of Pb(II) from aqueous solutions by LSH is largely reliant on the different polar functional groups, including hydroxyl, phenols, amines, and aromatics. The presence of polyphenols, including three flavones, one isoflavone (genistein), one dihydroflavonol derivative, and numerous hydroxybenzoic and hydroxycinnamic acid derivatives, is supported by the presence of −OH, −COOH, and $-NH_2$ groups on the surface of LSH which can interact with Pb(II).[41] Polar polyphenolic groups present on the LSH surface increase the LSH's ability to exchange cations.[42] If we designate the adsorbent as LSH, then eqs 18−20 could be used to represent the lead interaction on its surface.

$$\text{LSH-COOH} + \text{Pb(II)} = \text{LSH-COOPb(I)} + \text{H}^+ \quad (18)$$

$$\text{LSH-OH} + \text{Pb(II)} = \text{LSH-OPb(I)} + \text{H}^+ \quad (19)$$

$$\text{LSH-NH}_2 + \text{Pb(II)} = \text{LSH-NPb} + 2\text{H}^+ \quad (20)$$

Figure 14 summarizes the proposed Pb(II) adsorption mechanism on the LSH surface.

https://doi.org/10.1021/acsomega.3c05337
ACS Omega 2023, 8, 42622−42631

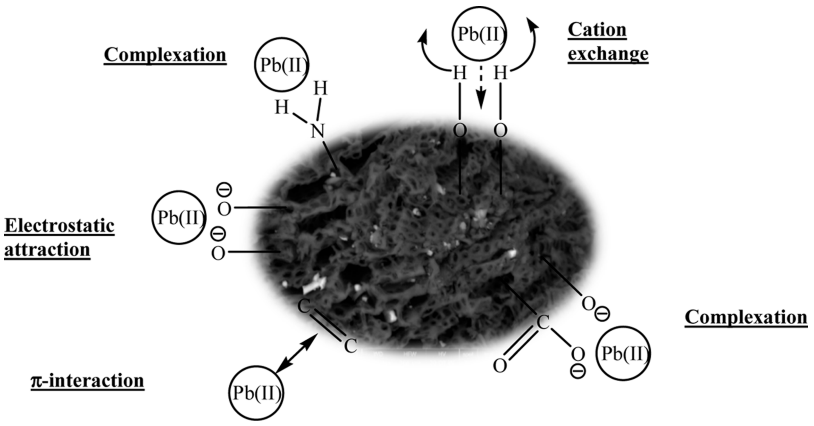

Figure 14. Possible reaction mechanisms for Pb(II) removal by LSH.

Strong forces have been demonstrated by the −COOH groups that bind Pb(II) ions through ion exchange and electrostatic interactions. Through complexation and electrostatic interactions, the active group ($-NH_2$) allowed LSH to quickly and effectively adsorb Pb(II) ions in aqueous solution.[43] The Pb(II) ions, which has the electronic configuration $4f^{14}$ $5d^{10}$ $6s^2$, could then be quickly complexed by nitrogen and oxygen lone pairs of LSH components to create a multitoothed complex.[44]

The maximal adsorption capacity of various biosorbents for the removal of Pb(II) from aqueous solutions is revealed by a literature review (Table 3). Table 3 compares the adsorption capacity of the LSH biosorbent to those of various similar biomasses, highlighting the feasibility of employing LSH for the uptake of Pb(II) ions from wastewater without any treatment or modification.

Table 3. Comparison Investigations of the Current Study and Previously Published Biosorbent Materials for Pb(II) Removal

adsorbent	dose, g	time, min	initial conc., C_o, mg/L	pH	max. capacity (mg/g)	refs
cucumber peel	1	60		5.0	133.6	5
native garlic peel		40		5.0	58.04	45
mercerized garlic peel		40		5.0	105.82	45
rape straw		15		3.0–4.0	253.2	46
mangosteen peel		180		5.0	130	12
peanut shells	1		100	3.5–5.5	39.0	47
coir pith waste		30		4.0	263.0	48
wheat bran		87		4.0–6.0	87.0	49
peels of banana	2			5.0	2.18	11
okra waste			240	5.0	5.0	50
rice husk	2			5.0	5.69	51
tea waste	0.5		5–100	5.0	73	52
Pinus nigra tree bark	2.5		35	8.0	49	53
lentil husk		60	250	5.0	81.43	54
modified Mangifera indica seed shells	0.5			5.2	306.33	55
LSH	0.4	60	50	5.5	357.14	this study

3.2.7. Reusability and Regeneration of LSH. From economic and environmental perspectives, adsorbent regeneration is significant. The adsorption process between the adsorbent and adsorbate can be better understood through regeneration studies.[56,57] Adsorbed Pb(II) creates a thin layer on the surface of LSH that may be dissolved effortlessly with HCl, so, 0.1 M HCl was used in the current work as a desorbing agent for regeneration.[56] To test how well the adsorbent can maintain its metal adsorption capacity, we utilized it again for further adsorption/desorption cycles. Figure 15 depicts the outcome of LSH-assisted Pb(II) adsorption. The efficiency of LSH was recycled for four continuous adsorption and desorption cycles, during which it dropped from 95.8 to 35.0%, demonstrating the viability of four iterations of adsorbent regeneration. The reduction in loading capacity after desorption may be caused by structural damage to the LSH, LSH loss, and metal complexes obstructing binding sites. According to reports, treating biomass with acids resulted in structural damage to the biomass.[58,59]

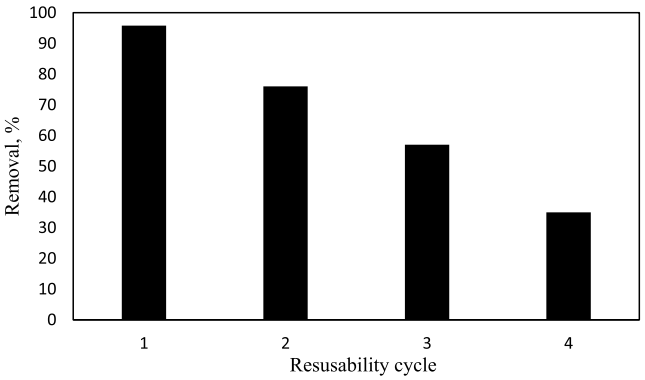

Figure 15. Regeneration of LSH for the removal of Pb(II).

3.2.8. Removal of Lead from Industrial Effluents. Actual effluent from a battery manufacturing facility in Cairo, Egypt, comprising 10.3 mg L^{-1} of lead and 10 mg L^{-1} of cadmium and chromium, was given to LSH for interaction. 0.4 g of the LSH was placed in 25 mL of the wastewater having lead,

https://doi.org/10.1021/acsomega.3c05337
ACS Omega 2023, 8, 42622−42631

cadmium, and chromium after adjusting the pH to 5.5. The content of Pb(II) in the effluent was successfully reduced to 0.6 mg L^{-1} by LSH whereas cadmium and chromium were not adsorbed on LSH, and their concentration is 9.8 and 9.0 mg L^{-1}, respectively. So, LSH is a selective adsorbent for Pb(II) from industrial wastewater.

4. CONCLUSIONS

For the first time, this work proposed using a naturally available and environmentally acceptable LSH as a new adsorbent to uptake Pb(II). The percentage of Pb(II) elimination was examined in relation to experimental variables, such as LSH dosage, pH, and interaction time. Using batch adsorption tests, the LSH adsorbent performed well for Pb(II) adsorption. SEM, EDX, FTIR, and BET analyses were used to determine the physicochemical and structural properties of LSH in order to learn about its chemical structure, functional groups, and surface area. The Langmuir isotherm model with a maximum adsorption capacity of 357.14 mg/g at optimized pH (5.5), LSH dose (0.4 g), and interaction time (60 min) was used. Pb(II) uptake by LSH has been shown to be best explained by pseudo-second-order kinetics. LSH could be reused for four consecutive cycles after sorbent regeneration with 0.1 M HCl. Therefore, LSH is a potent biosorbent for the uptake of Pb(II) from wastewater samples.

■ ASSOCIATED CONTENT

Supporting Information

The Supporting Information is available free of charge at https://pubs.acs.org/doi/10.1021/acsomega.3c05337.

Instrumental conditions for the measurement of lead by FAAS and N_2 adsorption−desorption isotherm of LSH (PDF)

■ AUTHOR INFORMATION

Corresponding Author

Awaad H. A. Aboterika − *Central Laboratory, Faculty of Science, Ain Shams University, 11566 Cairo, Egypt;* orcid.org/0000-0002-1993-3981; Email: awaad_2000@sci.asu.edu.eg

Authors

Amal A. Abdel Hafez − *Chemistry Department, Faculty of Science, King Khalid University, Abha 61421, Saudi Arabia*

Hisham S. M. Abd-Rabboh − *Chemistry Department, Faculty of Science, King Khalid University, Abha 61421, Saudi Arabia*

Ali M. Al-Marri − *Public Works Authority (ASHGHAL), 22188 Doha, Qatar*

Complete contact information is available at: https://pubs.acs.org/10.1021/acsomega.3c05337

Notes

The authors declare no competing financial interest.

■ ACKNOWLEDGMENTS

The authors extend their appreciation to the Deanship of Scientific Research at King Khalid University for funding this work through the Large Groups Project under grant no. RGP.2/335/44.

■ REFERENCES

(1) Vardhan, K. H.; Kumar, P. S.; Panda, R. C. A review on heavy metal pollution, toxicity and remedial measures: Current trends and future perspectives. *J. Mol. Liq.* **2019**, *290*, 111197.

(2) Sheth, Y.; Dharaskar, S.; Khalid, M.; Sonawane, S. An environment friendly approach for heavy metal removal from industrial wastewater using chitosan based biosorbent: A review. *Sustain. Energy Technol. Assess.* **2021**, *43*, 100951.

(3) Farooq, U.; Kozinski, J. A.; Khan, M. A.; Athar, M. Biosorption of heavy metal ions using wheat based biosorbents - a review of the recent literature. *Bioresour. Technol.* **2010**, *101*, 5043−5053.

(4) Schwantes, D.; Gonçalves, A. C.; Campagnolo, M. A.; Tarley, C. R. T.; Dragunski, D. C.; de Varennes, A.; dos Santos Silva, A. K.; Conradi, E. Chemical modifications on pinus bark for adsorption of toxic metals. *J. Environ. Chem. Eng.* **2018**, *6*, 1271−1278.

(5) Basu, M.; Guha, A. K.; Ray, L. Adsorption of lead on cucumber peel. *J. Cleaner Prod.* **2017**, *151*, 603−615.

(6) Nadeem, R.; Ansari, T. M.; Akhtar, K.; Khalid, A. M. Pb(II) sorption by pyrolysed Pongamia pinnata pods carbon (PPPC). *Chem. Eng. J.* **2009**, *152*, 54−63.

(7) Morosanu, I.; Teodosiu, C.; Paduraru, C.; Ibanescu, D.; Tofan, L. Biosorption of lead ions from aqueous effluents by rapeseed biomass. *New Biotechnol.* **2017**, *39*, 110−124.

(8) (a) Nguyen, T. A. H.; Ngo, H. H.; Guo, W. S.; Zhang, J.; Liang, S.; Yue, Q. Y.; Li, Q.; Nguyen, T. V. Applicability of agricultural waste and by-products for adsorptive removal of heavy metals from wastewater. *Bioresour. Technol.* **2013**, *148*, 574−585. (b) Bădescu, I. S.; Bulgariu, D.; Ahmad, I.; Bulgariu, L. Valorisation possibilities of exhausted biosorbents loaded with metal ions - A review. *J. Environ. Manage.* **2018**, *224*, 288−297.

(9) Oladoye, P. O. Natural, low-cost adsorbents for toxic Pb(II) ion sequestration from (waste) water: a state-of-the-art review. *Chemosphere* **2022**, *287*, 132130.

(10) Yahya, M. D.; Yohanna, I.; Auta, M.; Obayomi, K. S. Remediation of Pb (II) ions from Kagara gold mining effluent using cotton hull adsorbent. *Sci. Afr.* **2020**, *8*, No. e00399.

(11) Anwar, J.; Shafique, U.; Waheed-uz-Zaman Salman, M.; Salman, M.; Dar, A.; Anwar, S. Removal of Pb(II) and Cd(II) from water by adsorption on peels of banana. *Bioresour. Technol.* **2010**, *101*, 1752−1755.

(12) Kongsune, P.; Rattanapan, S.; Chanajaree, R. The removal of Pb^{2++} from aqueous solution using mangosteen peel activated carbon: isotherm, kinetic, thermodynamic and binding energy calculation. *Groundw. Sustain. Dev.* **2021**, *12*, 100524.

(13) Pehlivan, E.; Altun, T.; Cetin, S.; Iqbal Bhanger, M. Lead sorption by waste biomass of hazelnut and almond shell. *J. Hazard. Mater.* **2009**, *167*, 1203−1208.

(14) Iqbal, M.; Saeed, A.; Zafar, S. I. FTIR spectrophotometry, kinetics and adsorption isotherms modeling, ion exchange, and EDX analysis for understanding the mechanism of Cd^{2+} and Pb^{2+} removal by mango peel waste. *J. Hazard. Mater.* **2009**, *164*, 161−171.

(15) Gupta, V. K.; Carrott, P. J. M.; Ribeiro Carrott, M. M. L.; Suhas. Low-Cost adsorbents: growing approach to wastewater treatment a review. *Crit. Rev. Environ. Sci. Technol.* **2009**, *39*, 783−842.

(16) Oliveira, F. D.; Paula, J. H.; Freitas, O. M.; Figueiredo, S. A. Copper and lead removal by peanut hulls: Equilibrium and kinetic studies. *Desalination* **2009**, *248*, 931−940.

(17) Arsenie, T.; Cara, I. G.; Popescu, M.-C.; Motrescu, I.; Bulgariu, L. Evaluation of the Adsorptive Performances of Rapeseed Waste in the Removal of Toxic Metal Ions in Aqueous Media. *Water* **2022**, *14*, 4108.

(18) Kyzas, G. Z.; Mitropoulos, A. C. Zero-cost agricultural wastes as sources for activated carbons synthesis: lead ions removal from wastewaters. *Proceedings* **2018**, *2*, 652.

(19) Islam, S.; Ma, W. L. *Encyclopedia of Food and Health*; B., Caballero, P. M., Finglas, F., Toldrá, Eds.; Academic Press, 2016; pp 579−585.

https://doi.org/10.1021/acsomega.3c05337
ACS Omega 2023, 8, 42622−42631

(20) Alene, A. N.; Abate, G. Y.; Habte, A. T.; Getahun, D. M. Utilization of a novel low-cost Gibto Lupinus Albus seed peel waste for the removal of malachite green dye: equilibrium, kinetic, and thermodynamic studies. *J. Chem.* **2021**, *2021*, 1−16.
(21) Zhong, L.; Fang, Z.; Wahlqvist, M. L.; Hodgson, J. M.; Johnson, S. K. Multi-response surface optimisation of extrusion cooking to increase soluble dietary fibre and polyphenols in lupin seed coat. *LWT* **2021**, *140*, 110767.
(22) Rahmat, N. A.; Ali, A. A.; Salmiati; Hussain, N.; Muhamad, M. S.; Kristanti, R. A.; Hadibarata, T. Removal of remazol brilliant blue R from aqueous solution by adsorption using pineapple leaf powder and lime peel powder. *Water, Air, Soil Pollut.* **2016**, *227* (4), 105.
(23) Langmuir, I. (1918) The adsorption of gases on plane surfaces of glass, mica and platinum. *J. Am. Chem. Soc.* **1918**, *40* (9), 1361−1403.
(24) Munagapati, V. S.; Kim, D.-S. Adsorption of anionic azo dye congo red from aqueous solution by cationic modified orange peel powder. *J. Mol. Liq.* **2016**, *220*, 540−548.
(25) Lagergren, S. About the theory of so-called adsorption of soluble substances. *K. Sven. Vetensk. Akad. Handl.* **1898**, *24*, 1−39.
(26) Ho, Y. S. Review of second-order models for adsorption systems. *J. Hazard. Mater.* **2006**, *136*, 681−689.
(27) Weber, W. J.; Morris, J. C. Kinetics of Adsorption on Carbon from Solution. *J. Sanit. Eng. Div.* **1963**, *89*, 31−59.
(28) Yousefi, M.; Gholami, M.; Oskoei, V.; Mohammadi, A. A.; Baziar, M.; Esrafili, A. Comparison of LSSVM and RSM in simulating the removal of ciprofloxacin from aqueous solutions using magnetization of functionalized multi-walled carbon nanotubes: Process optimization using GA and RSM techniques. *J. Environ. Chem. Eng.* **2021**, *9*, 105677.
(29) Temesgen, F.; Gabbiye, N.; Sahu, O. Biosorption of reactive red dye (RRD) on activated surface of banana and orange peels: economical alternative for textile effluent. *Surf. Interfaces* **2018**, *12*, 151−159.
(30) Hashem, A.; Aniagor, C. O.; Badawy, S. M.; Taha, G. M. Novel application of the esterification product of 2,3-dihydroxybutanedioic acid and cellulosic biomass for cobalt ion adsorption. *Korean J. Chem. Eng.* **2021**, *38* (11), 2256−2264.
(31) Uddin, M. T.; Rahman, M. A.; Rukanuzzaman, M.; Islam, M. A. A potential low cost adsorbent for the removal of cationic dyes from aqueous solutions. *Appl. Water Sci.* **2017**, *7* (6), 2831−2842.
(32) Mondal, N. K.; Kar, S. Potentiality of banana peel for removal of Congo red dye from aqueous solution: isotherm, kinetics and thermodynamics studies. *Appl. Water Sci.* **2018**, *8* (6), 157.
(33) Munagapati, V. S.; Yarramuthi, V.; Kim, Y.; Lee, K. M.; Kim, D. S. Removal of anionic dyes (Reactive Black 5 and Congo Red) from aqueous solutions using Banana Peel Powder as an adsorbent. *Ecotoxicol. Environ. Saf.* **2018**, *148*, 601−607.
(34) Kuang, X.; Shao, J.; Peng, L.; Song, H.; Wei, X.; Luo, S.; Gu, J. D. Nano-TiO_2 enhances the adsorption of Cd (II) on biological soil crusts under mildly acidic conditions. *J. Contam. Hydrol.* **2020**, *229*, 103583.
(35) Vernè, E.; Nunzio, S. D.; Bosetti, M.; Appendino, P.; Vitale Brovarone, C.; Maina, G.; Cannas, M. Surface characterization of silver-doped bioactive glass. *Biomaterials* **2005**, *26* (25), 5111−5119.
(36) Negi, R.; Satpathy, G.; Tyagi, Y. K.; Gupta, R. K. Biosorption of heavy metals by utilising onion and garlic wastes. *Int. J. Environ. Pollut.* **2012**, *49*, 179−196.
(37) Jeyakumar, R. P. S.; Chandrasekaran, V. Adsorption of lead(II) ions by activated carbons prepared from marine green algae: equilibrium and kinetics studies. *Int. J. Ind. Chem.* **2014**, *5*, 10.
(38) Kypritidou, Z.; El-Bassi, L.; Jellali, S.; Kinigopoulou, V.; Tziritis, E.; Akrout, H.; Jeguirim, M.; Doulgeris, C. Lead removal from aqueous solutions by olive mill wastes derived biochar: Batch experiments and geochemical modelling. *J. Environ. Manage.* **2022**, *318*, 115562.
(39) Regti, A.; Laamari, M. R.; Stiriba, S.-E.; El Haddad, M. Potential use of activated carbon derived from Persea species under alkaline conditions for removing cationic dye from wastewaters. *J. Assoc. Arab Univ. Basic Appl. Sci.* **2017**, *24* (1), 10−18.
(40) Theydan, S. K.; Ahmed, M. J. Adsorption of methylene blue onto biomass-based activated carbon by FeCl3 activation: Equilibrium, kinetics, and thermodynamic studies. *J. Anal. Appl. Pyrolysis* **2012**, *97*, 116−122.
(41) Zhong, L.; Wu, G.; Fang, Z.; Wahlqvist, M. L.; Hodgson, J. M.; Clarke, M. W.; Junaldi, E.; Johnson, S. K. Characterization of polyphenols in Australian sweet lupin (Lupinus angustifolius) seed coat by HPLC-DAD-ESI-MS/MS. *Food Res. Int.* **2019**, *116*, 1153−1162.
(42) Abdel-Ghani, N. T.; Hegazy, A. K.; El-Chaghaby, G. A. Typha domingensis leaf powder for decontamination of aluminium, iron, zinc and lead: Biosorption kinetics and equilibrium modeling. *Int. J. Environ. Sci. Technol.* **2009**, *6* (2), 243−248.
(43) Li, W.; Ju, B.; Zhang, S. A green l-cysteine modified cellulose nanocrystals biosorbent for adsorption of mercury ions from aqueous solutions. *RSC Adv.* **2019**, *9* (12), 6986−6994.
(44) Farkas, E.; Buglyo, P. Lead(II) Complexes of Amino Acids, Peptides, and Other Related Ligands of Biological Interest. *Met. Ions Life Sci.* **2017**, *17*, 201−240.
(45) Liu, W.; Liu, Y.; Tao, Y.; Yu, Y.; Jiang, H.; Lian, H. Comparative study of adsorption of Pb(II) on native garlic peel and mercerized garlic peel. *Environ. Sci. Pollut. Res.* **2014**, *21*, 2054−2063.
(46) Zhang, Z.; Wang, T.; Zhang, H.; Liu, Y.; Xing, B. Adsorption of Pb(II) and Cd(II) by magnetic activated carbon and its mechanism. *Sci. Total Environ.* **2021**, *757*, 143910.
(47) Taşar, Ş.; Kaya, F.; Özer, A. Biosorption of lead(II) ions from aqueous solution by peanut shells: equilibrium, thermodynamic and kinetic studies. *J. Environ. Chem. Eng.* **2014**, *2*, 1018−1026.
(48) Kadirvelu, K.; Namasivayam, C. Agricutural By-Product as Metal Adsorbent: Sorption of Lead(II) from Aqueous Solution onto Coirpith Carbon. *Environ. Technol.* **2000**, *21*, 1091−1097.
(49) Bulut, Y.; Baysal, Z. Removal of Pb(II) from wastewater using wheat bran. *J. Environ. Manag.* **2006**, *78*, 107−113.
(50) Hashem, M. A. Adsorption of lead ions from aqueous solution by okra wastes. *Int. J. Phys. Sci.* **2007**, *2*, 178−184.
(51) Zulkali, M. M. D.; Ahmad, A. L.; Norulakmal, N. H.; Sharifah, N. S. Comparative studies of Oryza sativa L. husk and chitosan as lead adsorbent. *J. Chem. Technol. Biotechnol.* **2006**, *81*, 1324−1327.
(52) Ahluwalia, S. S.; Goyal, D. Removal of heavy metals by waste tea leaves from aqueous solution. *Eng. Life Sci.* **2005**, *5*, 158−162.
(53) Argun, M. E.; Dursun, S. Activation of pine bark surface with NaOH for lead removal. *J. Int. Environ. Appl. Sci.* **2007**, *2*, 5−10.
(54) Basu, M.; Guha, A. K.; Ray, L. Biosorptive removal of lead by lentil husk. *J. Environ. Chem. Eng.* **2015**, *3* (2), 1088−1095.
(55) Moyo, M.; Pakade, V. E.; Modise, S. J. Biosorption of lead(II) by chemically modified Mangifera indica seed shells: Adsorbent preparation, characterization and performance assessment. *Process Saf. Environ. Prot.* **2017**, *111*, 40−51.
(56) Pawar, S.; Bagali, S.; Uma, K.; Gowrishankar, B. S. Column study using modified banana pseudo stem as adsorbent for removal of Pb(II). *Heliyon* **2023**, *9* (5), No. e15469.
(57) Sharma, P.; Iqbal, H. M.; Chandra, R. Evaluation of pollution parameters and toxic elements in wastewater of pulp and paper industries in India: A case study. *Case Stud. Chem. Environ. Eng.* **2022**, *5*, 100163.
(58) Saeed, A.; Iqbal, M. Bioremoval of cadmium from aqueous solution by black gram husk (Cicer arientinum). *Water Res.* **2003**, *37* (14), 3472−3480.
(59) Tsezos, M. Recovery of uranium from biological adsorbents-desorption equilibrium. *Biotechnol. Bioeng.* **1984**, *26*, 973−981.

https://doi.org/10.1021/acsomega.3c05337
ACS Omega 2023, 8, 42622−42631